Journal of Manufacturing Processes 28 (2017) 541–549

Contents lists available at ScienceDirect

Journal of Manufacturing Processes

journal homepage: www.elsevier.com/locate/manpro

45th SME North American Manufacturing Research Conference, NAMRC 45, LA, USA

Highly removable water support for Stereolithography

Jie Jin, Yong Chen*

Daniel J. Epstein Department of Industrial and Systems Engineering, University of Southern California, Los Angeles, CA, 90089, USA

ARTICLE INFO

Article history:
Received 18 November 2016
Accepted 3 March 2017
Available online 29 April 2017

Keywords:
Stereolithography
Additive manufacturing
Support structure
Ice
Projection

ABSTRACT

Current stereolithography (SL) technology can print there-dimensional (3D) objects with high precision and fast speed. However, for a complex computer-aided design (CAD) model, the fabricated structures have a significant amount of additional support structures that are required in order to ensure the model can be fabricated. However, these support structures may be difficult to remove. Even worse, the removal of the support structures may cause unexpected damage to delicate features and leave undesired surface marks. Although some special materials have been utilized in support structures such as water-soluble materials for the fused deposition modeling (FDM) process and wax for the multi-jet modeling (MJM) process, such support materials have not been available for the SL process. In this paper, a novel SL process using highly removable and widely available water as supports is presented. The process uses solid ice to surround the built parts in the layer-by-layer fabrication process. A cooling device is used to freeze the water into ice for each layer. The photocurable resin is spread on ice surface and then solidified by a projection image. Accordingly, a complex 3D object can be fabricated without using traditional support structures. After the fabrication process, the additional ice structure can easily be removed leaving no undesired marks on the bottom surfaces. Two test cases are presented to show the effectiveness of the presented highly removable water support method.

1. Introduction

In ancient time, some types of trees can produce resin. The abnormal development of resin in living trees can result in the formation of amber. Amber is fossilized tree resin, which has been appreciated for its color and natural beauty for a long time. Amber sometimes contains animal and plant material as inclusions, especially when the resin dropped onto the ground. Hence an insect may be surrounded by this unexpected tree resin. Over time, the resin may survive long enough to become amber and the insect pose inside will last forever [1]. Inspired by this phenomenon in nature, we hope to apply the amber mechanism to additive manufacturing (AM) process for support structures.

Layer-based AM processes, such as stereolithography (SL) [2], can directly fabricate parts from CAD models. As a direct digital manufacturing approach, current AM processes can effectively fabricate extremely complex three-dimensional (3D) shapes that used to be impossible to be made [3]. However, for most CAD models with complex geometries, extra support structures are needed in the layer-based fabrication process [4,5]. For the fused deposition modeling (FDM) process, some special water-soluble materials have been invented to print support structures by choosing multi-material printing mode [6]; people also used wax material as the support structures in the multi-jet modeling (MJM) process [7]. Consequently, removing support structures becomes easier and it is less likely to damage the built parts when removing the support structures. However, for the SL process, the building process uses a liquid resin tank. Hence, the SL process based on multi-materials has always been difficult although some previous efforts have been made to achieve multi-material SL process [8–11].

We are motivated to address this critical challenge for the SL process. In this research, we investigate the fabrication process based on water/ice for the mask-image-projection based stereolithography (MIP-SL) [12,13]. In the MIP-SL process, a CAD model is sliced into a set of two-dimensional (2D) layers with a given layer thickness. Each layer is prepared individually by projecting the masked image of the layer onto the liquid resin surface. After the ultraviolet (UV) light exposure, liquid resin is solidified into the sliced layer shape that attaches to the previous layers. In order to add water support structure, we investigate the top-down projection system in the MIP-SL process. A critical thermoelectric device [14,15] is selected and applied in the MIP-SL system to freeze the water into ice.

Peer-review under responsibility of the Scientific Committee of NAMRI/SME.
* Corresponding author.
E-mail address: yongchen@usc.edu (Y. Chen).

http://dx.doi.org/10.1016/j.jmapro.2017.04.023
1526-6125/

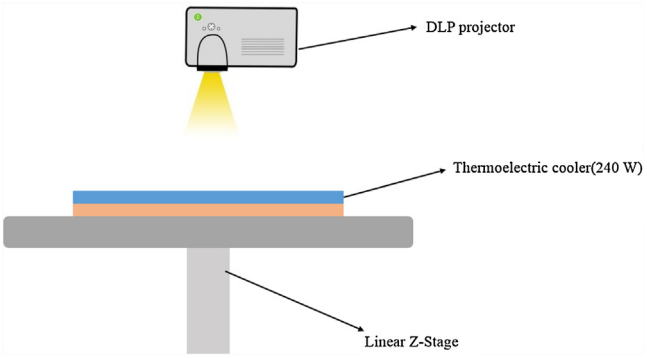

Fig. 1. Building platform for the process.

1.1. Limitations of traditional support structures for SL process

In the traditional SL process, the additional support structures will waste a lot of extra materials since they will be removed after finishing the building process. In addition, it is time-consuming for users to manually remove all the support structures. Even worse, the removal of the support structures may cause unexpected damage to delicate features of the built objects, resulting in undesired surface finish. Consequently, the added support structures will dramatically increase the building time and cost in addition to the tedious post-processing process. For some special applications, it may even be impossible to remove the support structures that are difficult to access, and support structures may be required in some critical areas that are not allowed to have them.

1.2. Contributions

To address the limitations of traditional support structures in the SL process, we present a novel approach to build water support that will surround the built objects in each layer. Our approach is a multi-material printing method based on a top-down projection system. We address the related challenges in controlling the surface level of ice due to the volumetric expansion when water converts to ice and other considerations. By optimizing the process settings, we have designed test cases to illustrate that our approach is able to fabricate critical components with delicate features. Consequently, the developed water-support-based MIP-SL process can fabricate highly complex parts which are previously impossible for the SL process.

2. Water support building process study

In this research, a top-down MIP-SL process is applied for building water support structures. However, unlike the traditional top-down SL process based on free surface, the top resin surface is constrained by a Teflon-coated transparent glass in our approach. In addition, instead of using a tank to store liquid resin, we adopt a material spreading and removing method to achieve the desired water support building process. Consequently, the final building part will be surrounded by solid ice similar to Amber, instead of fixing by additional supports that are merged inside liquid resin tank.

2.1. Building platform design

As shown in Fig. 1, a thermoelectric cooler is mounted on a linear *Z*-stage, which can move up and down along the *Z* direction. The thermoelectric cooler in our setup is used as the building platform where the built layers will be grown from. When a positive voltage is applied to the thermoelectric cooler, the temperature on the top surface will dramatically decrease to below zero degrees Celsius just in seconds. Thus, it can maintain a continued low temperature environment to ensure the success of the building process. Consequently, the thermoelectric cooler that is used as a building platform will always be kept on during the entire building process until all the layers have been built.

2.2. Building process illustration

A water dispenser is mounted on the front of tool *A* as shown in Fig. 2a. Adjusting the linear *Z*-stage to form a 100 μm gap between the top and bottom cooler, then we move tool *A* to spread one layer of water in a given thickness on the top surface of the bottom cooler. Due to the surface tension, water will be constrained in the gap between the two coolers. After turning on both of the two coolers, the water in the gap will be converted into ice in several seconds as shown in Fig. 2b. The bottom surface of the top cooler is coated with a piece of Teflon film in order to decrease its surface friction such that the top cooler can easily be separated from the ice below. The reason for building the first ice layer is for the easy separation of the part after the entire building process has been finished, i.e. the built object can easily be taken away from the building platform by simply melting the base ice layer. No extra effort is required. It will significantly prevent the built objects from being damaged by using a scraper in the traditional approach.

As shown in Fig. 2c, another tool *B* will move towards the building platform right after moving away from tool *A*. Similar to tool *A*, a resin dispenser is mounted on the front of tool *B*, which will be used to spread one-layer liquid resin on previously solidified layer surface with a desired layer thickness. After that, a pattern image is projected on the resin surface through a transparent glass. The exposure time for each layer in our setup is ~20 s.

A resin vacuum is mounted on the rear side of tool *B*. After the exposure time as shown in Fig. 2d, tool *B* is moved away. During the movement of tool *B*, the mounted resin vacuum will be turned on to suck out all the unsolidified residual liquid resin from the building platform, leaving only one layer of solidified resin pattern. After that, tool *A* will move towards the building platform again as shown in Fig. 2e. It will spread water to fill the empty slots in the previous layer and freeze them to ice. Consequently, we will get a layer that consists of both the solidified resin pattern and solidified ice. Then by repeating the process from Fig. 2c–e, another patterned layer as shown in Fig. 2g can be fabricated.

The flow chart shown in Fig. 3 briefly describes the water support building process.

2.3. A proof of concept

As shown in Fig. 4a, a simple CAD model was designed to verify the concept of the presented building process. Unlike the traditional SL process, which will require a support structure as shown in Fig. 4b for this CAD model, to ensure the success of the building process, we used the aforementioned process to directly fabricate the designed CAD model without adding any support structures. Instead, ice support similar to amber is added in the building process as shown in Fig. 4d. After finishing the building process, the surrounded ice support was then melted away as shown in Fig. 4e–f. Consequently, the desired part can be fabricated without any undesired surface marks as shown in Fig. 4g–i.

2.4. Study of the impact of ice on dimensional accuracy

The presented ice support building process requires the built part to be embedded in ice. Since water expands when it freezes, a study of the dimensional accuracy of a built part has been performed to understand the impact of ice and low temperature on

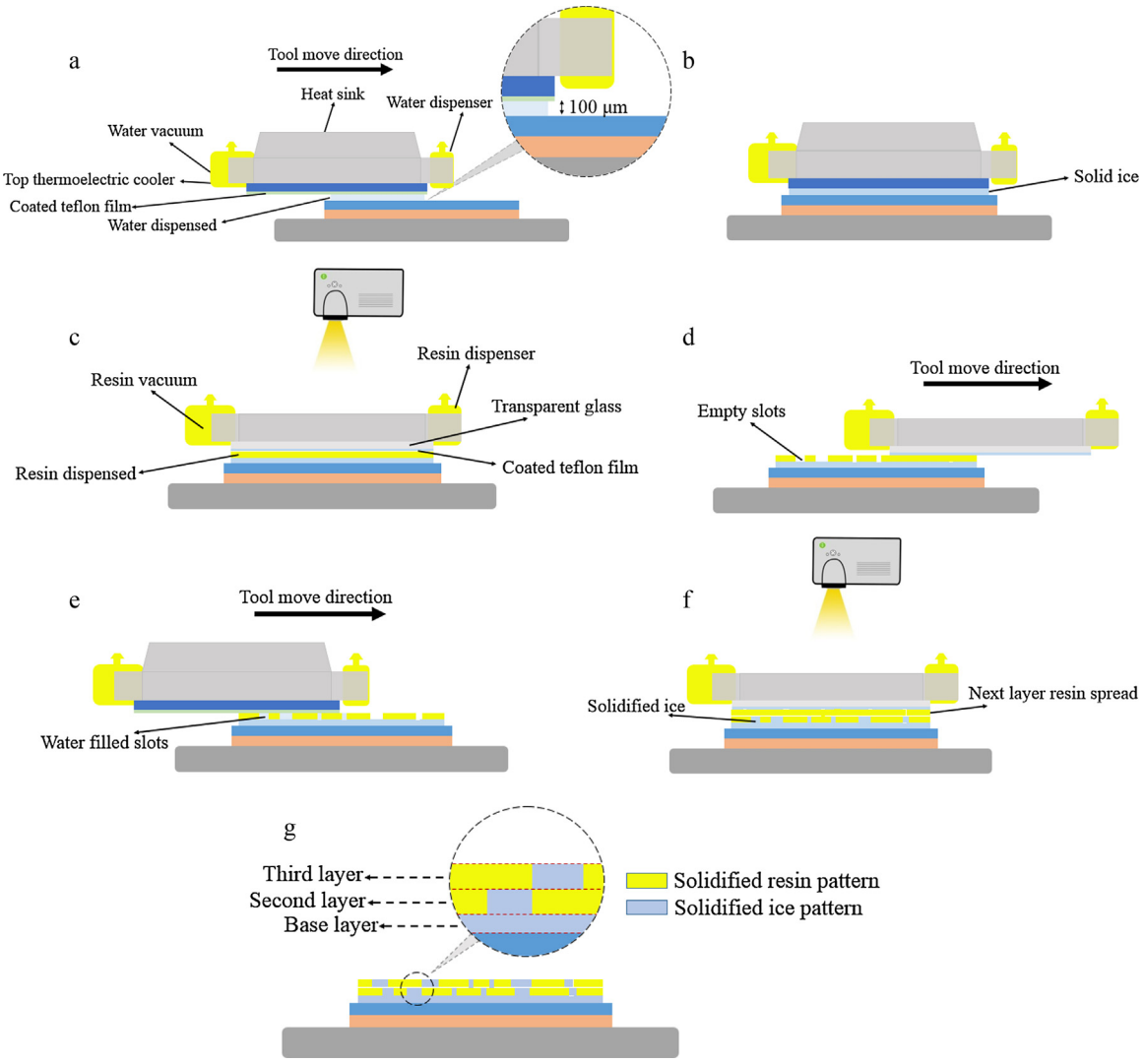

Fig. 2. A schematic illustration of the water support building process.

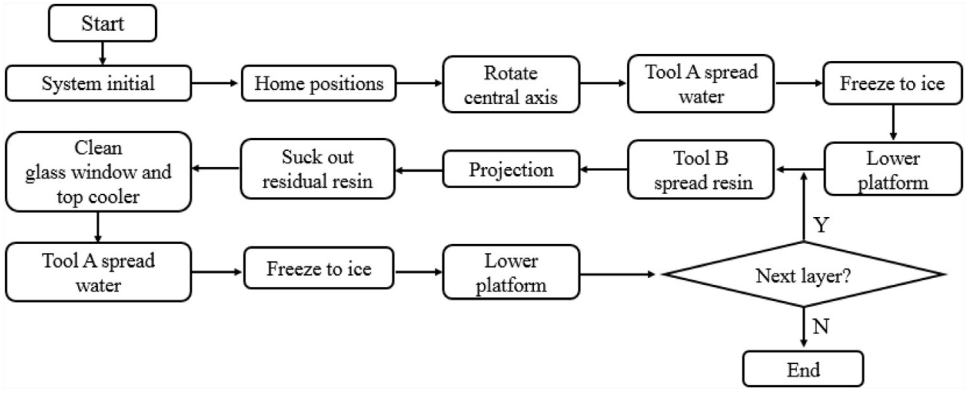

Fig. 3. Flow chart description of the water support building process.

the fabrication accuracy. The CAD model used in the study is a simple cube whose dimension is 20 mm × 20 mm × 2.5 mm. Two experimental factors are studied, which are the use of ice and low temperature as shown in Table 1. Each treatment has 3 runs and the observation data are the three dimensional sizes and the weight of each built part. A digital caliper is used to measure the dimensions. We measure 10 times in different sections along the same dimension. Each dimensional data as shown in Table 2 is the mean of the 10 measurements. In this study, every part is built in the same position along with the same bounding wall (introduced in Section 3.4) and the resin is applied in the first layer for each part.

By comparing treatment 1 (Ice – & Temperature –) with treatment 2 (Ice – & Temperature +), we can conclude that the temperature will not affect the dimensional accuracy since the data

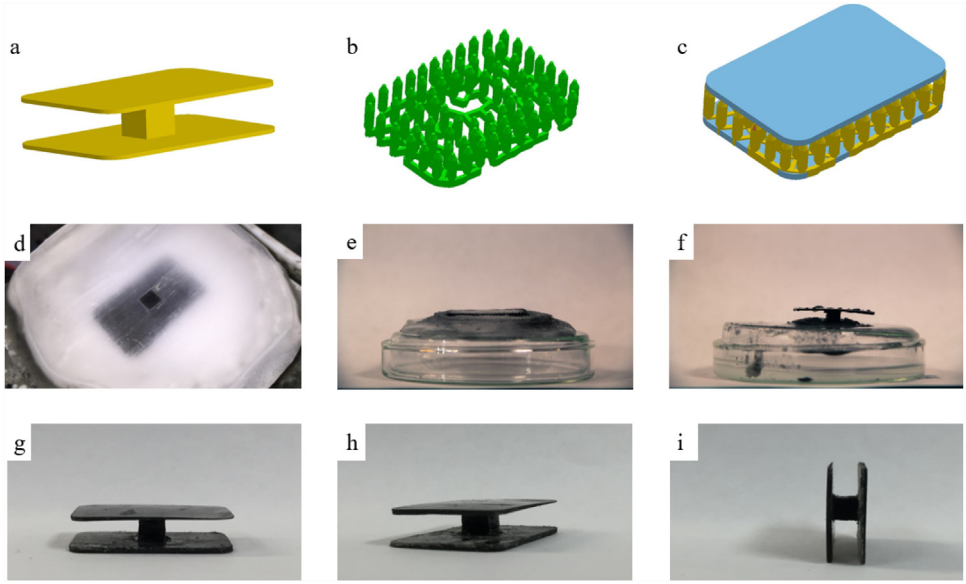

Fig. 4. A proof of concept. (a) A designed CAD model; (b) and (c) support structures that are required in the traditional SL process; (d) printing in process using water support; (e) and (f) melting the surrounded ice after the building process; and (g)–(i) the fabricated object in different views.

Table 1
Factors and levels, study of ice impact to dimensional accuracy.

Factors	Levels	
	–	+
Ice	Without ice	With ice
Temperature	Room temperature (~22 °C)	Low temperature (~−5 °C)

between treatment1 and treatment 2 are approximately the same. By comparing treatment 2 (Ice – & Temperature +) with treatment 3 (Ice + & Temperature +), we can conclude that ice will not affect the dimensional accuracy since the data between treatment 3 and treatment 2 are approximately the same. However, the particular photopolymer we investigate in the study, MakerJuice G plus, is just one of the candidates. The ice and temperature impact to other photopolymers will be studied in our future research.

In the *X* and *Y* dimensions, there is about 1 mm dimensional error between the designed model and the built part for all runs. This might be caused by the projector scale calibration error. In the *Z* dimension, there is about 0.1 mm dimensional error between the designed model and the built parts for all the runs. This error might be from the base layer because we calibrated the horizontal bottom surface of the building glass window as shown in Fig. 2c. However, the top surface of the building platform is not adjustable as shown in Fig. 1. Hence, the gap between the bottom surface of the building glass window and the top surface of the building platform at the very beginning will be a little bigger than the desired 100 μm layer thickness.

In short, we can conclude from the dimensional study that the use of ice and low-temperature shows an insignificant impact to the dimensional accuracy of the original part. This is reasonable because we dispense the water after liquid resin is solidified as shown in Fig. 2d and e. The material used in this study is rigid after it is solidified. Assuming the ice expansion force is homogeneous in each dimension, the ice expansion force applied to each dimension of the part is symmetrical. Hence, the defects due to ice expansion will be insignificant if the solidified material is reasonably rigid.

3. Ice surface level control

An interesting phenomenon we observed in our initial experiments indicates that the actual building layer thickness is much larger than what is expected for the layers. Even worse, some cured resin layers cannot be attached well to the previously built layers. After analyzing the entire building process, we determine that the water dispensing process as shown in Fig. 2e may cause the problem. Detailed analysis is discussed in Section 3.1 and the solution to address the problem is presented in Section 3.2. Consequently, the layer thickness can be under control after applying the solution in the experimental cases. A strategy to enhance the maximum building Z height is also introduced in Section 3.4 .

Table 2
Study of the impact of ice on dimensional accuracy.

Run	Factors		Dimension			Weight (g)	Mean			
	Ice	Temp.	X (mm)	Y (mm)	Z (mm)		X (mm)	Y (mm)	Z (mm)	Weight (g)
1	–	–	19.00	19.04	2.67	1.133	19.02	19.03	2.65	1.125
2	–	–	19.03	18.99	2.62	1.116				
3	–	–	19.02	19.06	2.65	1.125				
4	–	+	19.05	19.00	2.64	1.126	19.05	19.02	2.63	1.124
5	–	+	19.03	19.04	2.62	1.118				
6	–	+	19.06	19.01	2.64	1.129				
7	+	+	19.06	19.05	2.61	1.121	19.05	19.04	2.63	1.124
8	+	+	19.03	19.04	2.62	1.127				
9	+	+	19.05	19.02	2.65	1.123				

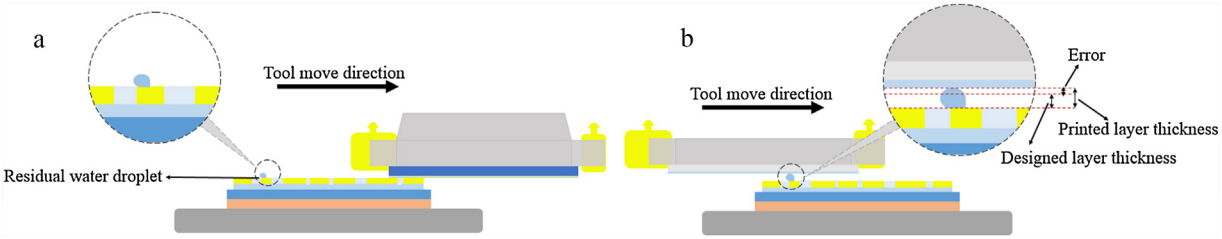

Fig. 5. An illustration of the building height stretch problem. (a) Residual water droplet left on the building surface; (b) ice ball pushes up tool *B*.

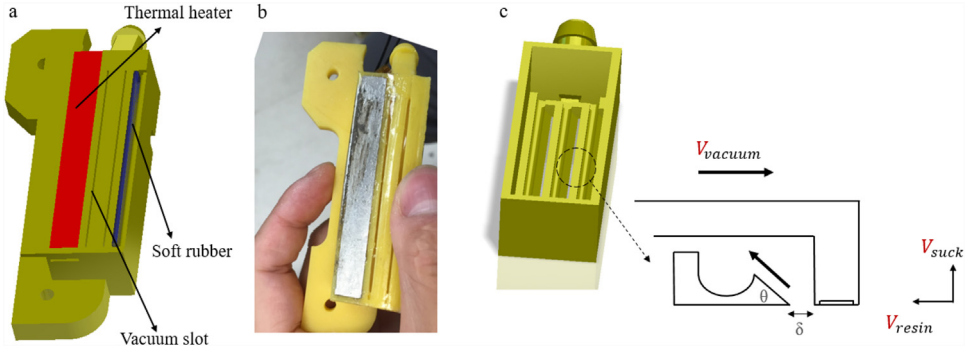

Fig. 6. A water vacuum design. (a) The CAD model of the designed water vacuum; (b) the fabricated water vacuum; and (c) the internal structure of the vacuum design.

3.1. Analysis of the height stretch problem

As studied in physics, the volume of water will be 10% larger when liquid water is converted into solid ice. However, it is obvious that the phenomenon that we observed from our initial experiments is much worse than this value. One scenario as shown in Fig. 5a is that some unexpected residual water droplets will remain on the building surface when tool *A* moves away from the building platform.

The residual water droplet may be taken from the rear edge of tool *A*. However, the water droplet will soon be frozen to a solid ice ball due to the low temperature environment. Such ice ball will stick on the top of the building surface. Hence when the next motion cycle begins, tool *B* will be pushed up when it passes through these ice balls. If the height of these ice balls are much bigger than the designed layer thickness as shown in Fig. 5b, the cured resin height on this layer will be much larger than the given layer thickness, resulting in the accumulated height that has a large error when the process is repeated.

Another scenario is that when tool *A* is applied to the building surface as shown in Fig. 2e, the bottom surface of the top cooler cannot guarantee seamless attachment with the previous layers because the previous layer surface is formed by another tool. That is, it may leave a rather thin ice layer on the top of building surface after tool *A* moves away from the building platform. So when next resin layer comes, it will not be able to attach to the previously built layers due to the existing extra intermediate thin ice layer between them.

3.2. Solution developed to control the surface level

The two problems as discussed in Section 3.1 are all caused by a common reason, i.e. the residual ice. A developed solution that is presented in this section will focus on how to efficiently remove such residual ice on the top building surface including both small ice balls and residual thin ice layer. We propose a water vacuum design as shown in Fig. 6 to address the problem. A thermal heater is mounted on the bottom surface that is used to preheat the residual ice droplets or thin ice layer. Thus, the residual molten ice can be easily sucked out via the vacuum slots of a water vacuum device. A temperature sensor is also applied to the bottom surface generating a closed-loop control of the heating temperature. The appropriate temperature used in our experiment is 40 °C. A soft rubber blade is also integrated with the water vacuum, which is embedded on the rear side of the vacuum. The rubber is about 0.5 mm higher than the bottom surface of the vacuum. The purpose of the rubber blade is to clean all the residual molten ice that is missed by the water vacuum head.

As shown in Fig. 6c, a parametric design model is developed, which allows us to use experiments to determine the following critical parameters for the vacuum structure, including vacuum slot width δ, slot angle θ, and moving speed V_{vacuum}.

- Vacuum slot width δ: This slot is designed to suck in the residual liquid water. The slot width is a vital factor to affect the vacuum sucking force. In our experiment, we have tried the width from 0.2 mm to 2 mm, and found that 0.2 mm is the most efficient one;
- Moving speed V_{vacuum}: In our experiments, the optimum V_{vacuum} is found to be 15 mm/s. The maximum speed that the rotary stage can achieve is 30 mm/s. Due to the time required for heat transfer between the thermal heater and the ice residues, the optimum value is chosen by balancing the maximum heat transferring time and the minimum building time;
- Slot angle θ: the designed slot angle θ is constrained to $\theta \leq \tan^{-1}\frac{V_{suck}}{V_{vaccum}}$, where V_{suck} denotes the speed of sucking air flow and is determined by the air pump and the slot width δ. The vacuum requires certain rigidity so that θ cannot be set to a very small value. In our experiment, θ is set to 45°.

3.3. Evaluation of the designed water vacuum

The improvement on the cleaning efficiency using the water vacuum as discussed in Section 3.2 is obvious. The height increase problem as discussed in Section 3.1 has been solved. The improvement is illustrated in Fig. 7.

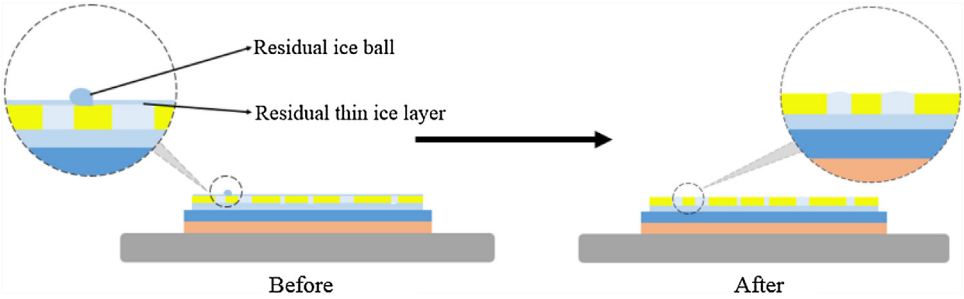

Fig. 7. Effect illustration of the efficient designed water vacuum.

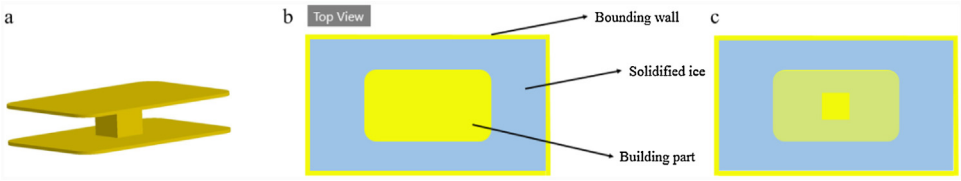

Fig. 8. (a) A test case of the designed CAD model to be built; (b) a top view of the built layers with ice at the initial few layers; and (c) a top view of the built layers with ice in the middle of the CAD model.

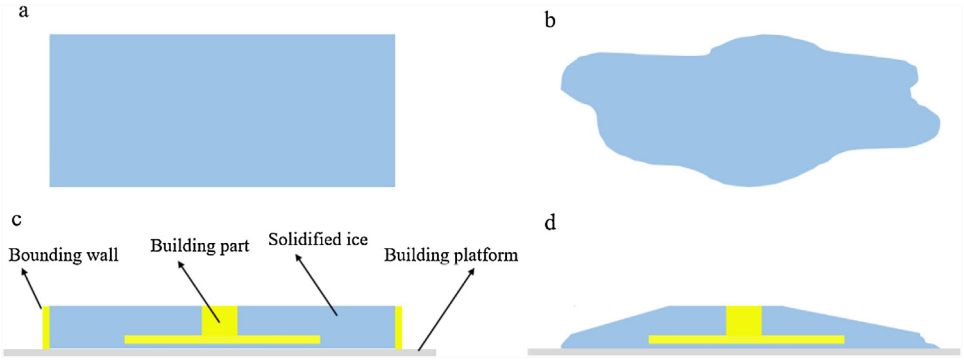

Fig. 9. The difference between using a bounding wall and without using the bounding wall. (a) Top view of the rectangular ice boundary when the bounding wall is applied; (b) top view of the irregular ice boundary without using the bounding wall; and (c)–(d) cross section views of with and without a bounding wall, respectively.

3.4. The strategy to enhance the building height

In the building process, we introduce an artificial bounding wall to enhance the ability of building relatively high parts in the *Z* direction, as shown in Fig. 8.

The designed bounding wall will have a certain distance offset from the boundary of the input CAD model. The bounding wall is built together with the model that is being fabricated. The purpose of the bounding wall is to constrain the deposited water to surround the sliced layers, preventing it from spreading towards the boundary of the building platform. In comparison, without the bounding wall, the cross section shape of the solidified ice will have a pyramid effect that can be observed from the experiments, resulting in the limited printing height that can be achieved as shown in Fig. 9d.

4. Experimental hardware and software systems

4.1. Hardware system

A prototype system has been built to verify the developed building process. The hardware setup of the water-support-based SL system is shown in Figure 10. In the designed system, an ultraviolet (UV) light projector is used. The wavelength of the light source is 405 nm. The power consuming of the light source is ~7 W. The projection resolution of the projector is 1280 × 800 and the building platform size is 62 mm × 62 mm. A precise linear stage from *Parker Inc.* is used as the elevator to drive the building platform in the *Z* axis. A precise rotary stage from *Parker Inc.* is used as the actuator for rotating the water dispensing tool and the resin dispensing tool. A high performance 4-axis motion controller with 28 GPIOs from *Dynomotion Inc.* (*Calabasas*, *CA*) is used to drive the steppers on the stages. Two critical thermoelectric devices are used to control the freezing of water to ice from bottom and top. And the electrical architecture of the hardware system is shown in Fig. 11.

4.2. Software system

The software system used in the experiments is developed using C ++ language with Microsoft Visual C ++ complier. The software integrates the geometry slicing and motion control features. It also coordinates the sliced images projection with the motion movements as well as the control of pumps and the thermoelectrical coolers. The graphical user interface of the developed software is shown in Fig. 12.

4.3. Material selection

MakerJuice G plus from *Makerjuice labs* is used in the experiments. This type of resin is selected since it is not sensitive to the temperature change and can work on the temperature range used in our study.

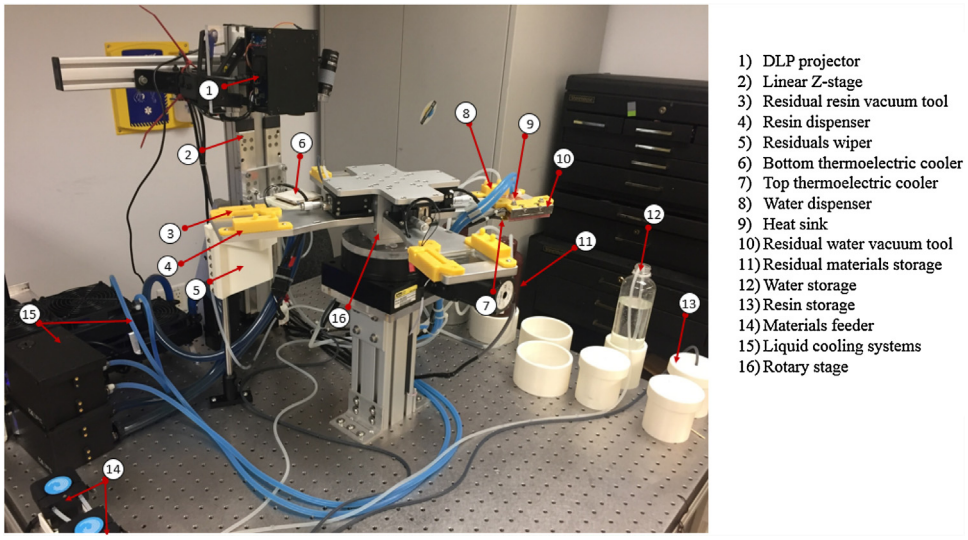

Fig. 10. The prototype hardware system for water support building process.

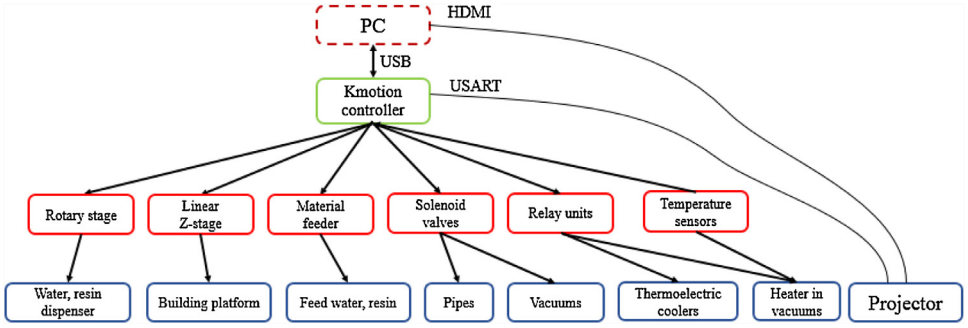

Fig. 11. The electrical architecture of the hardware system.

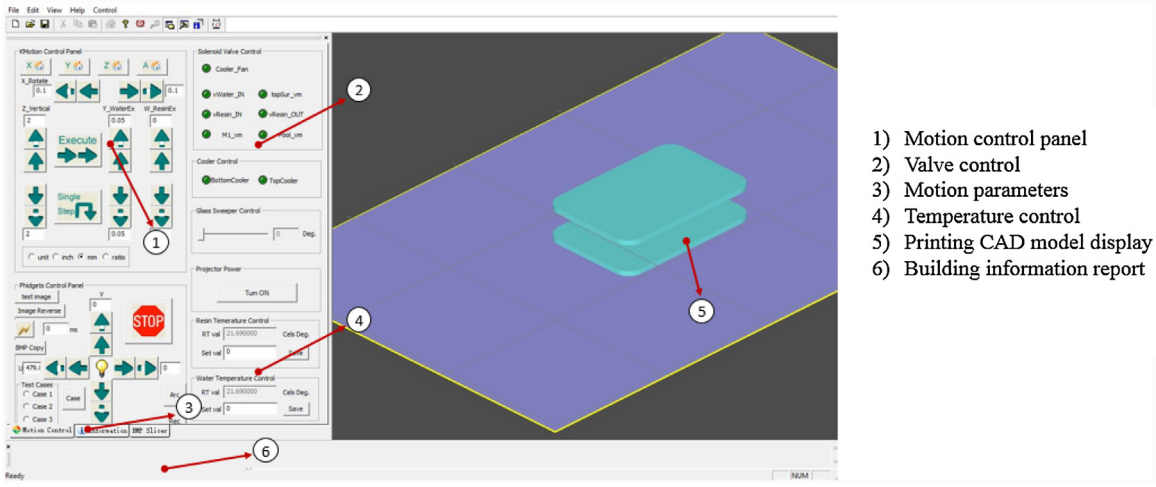

Fig. 12. Software system user interface.

5. Results and discussion

5.1. 3D ant with ice support

A 3D ant as shown in Fig. 13 was built to verify the water-support-based SL process in building delicate features. In the building process, the building direction of the test case is from legs to body. As shown in the building results in Fig. 14, the surrounded ice support presents two main benefits. Firstly, the ice support is highly removable that requires a minimum post-processing effort. Secondly and more importantly, the ice support can prevent delicate features from being damaged by constraining them during the printing process while adding no force to them when the ice support is removed after the building process.

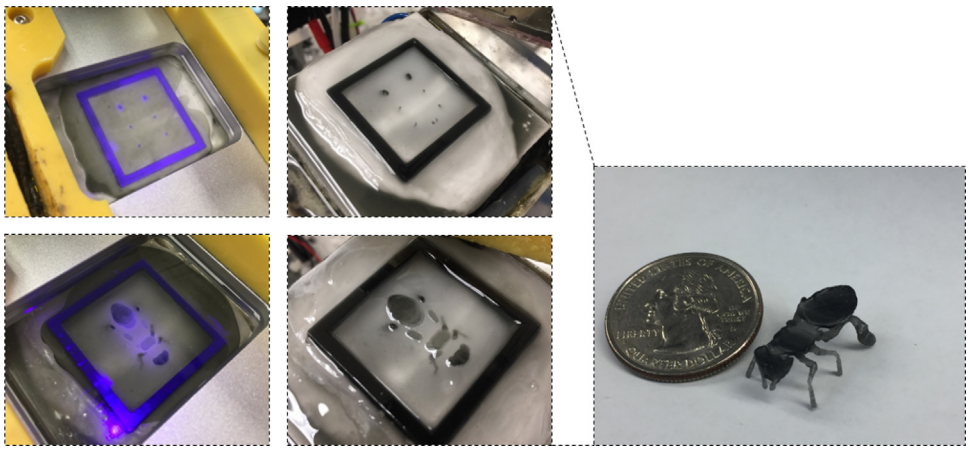

Fig. 13. The building process and result of the 3D ant.

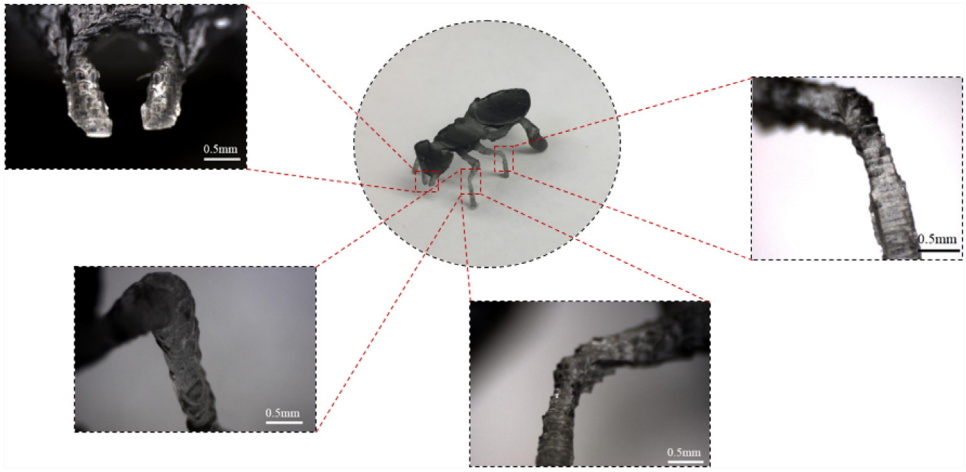

Fig. 14. The built 3D ant after removing ice in microscopic view.

5.2. Limitations and challenges

The presented water-support-based SL process has been demonstrated to fabricate general shapes and parts with delicate features using our experimental setup. However, several issues and potential challenges have also been identified during the experiments that will be addressed in our future work.

- *Bonding strength between layers.* Since the building process is implemented in a relatively low temperature environment, we have not tested the bonding force between difference layers with varying temperature conditions. The temperature impact to the bonding strength is still unknown (i.e. layer bonding becomes stronger, weaker, or remaining the same). The bonding strength may be a potential problem for building structural parts.
- *Materials selection.* Most of liquid resins available in the market have a high viscosity as temperature decreases. It is more difficult to spread them in the experiments. Hence the choice of appropriate resins for the presented process is reduced. The modification of resin with chemical solution to address the low-temperature building environment needs to be investigated.

6. Conclusion

A new stereolithography process based on highly removable water support structure has been presented. Thermoelectric devices have been incorporated in the building process so that liquid water can be frozen to ice in the layer-based building process. Since water or ice residues will significantly affect the curing process of spreading liquid resin, it is critical to control the ice surface level to ensure the success of the printing process. Our study introduces a novel design of vacuum tool with a heater to sufficiently remove the residual ice that is left on the building surface. An experimental prototype system has been built, which integrates various hardware and software components. Some representative test cases based on the prototyping system are presented to verify the capabilities of the water-support-based SL process in building challenging geometric features. Potential applications for the new AM process including microfluidic devices, which are under investigation.

Considerable work remains to mature the developed process and the correspondingly developed 3D printing system. Some future work that we are investigating includes: (1) developing multi-layer microfluidic devices with extremely complex channel paths; and (2) exploring applications that are enabled by our water-support-based SL process.

Acknowledgement

The work was partially supported by NSF CMMI-1151191.

References

[1] Poinar Jr GO. Life in Amber. Stanford, CA: Stanford University Press; 1991.

[2] Jacobs P. Rapid prototyping & manufacturing: fundamentals of stereolithography. Soc Manuf Eng 1992.
[3] Gao W, Zhang Y, Ramanujan D, Ramani K, Chen Y, Williams CB, et al. The status, challenges, and future of additive manufacturing in engineering. Comput Aided Des 2015;69:65–89.
[4] Chen Y, Li K, Qian X. Direct geometry processing for tele-fabrication. ASME J Comput Inf Eng 2013;13(4):041002.
[5] Huang P, Wang CCL, Chen Y. Algorithms for layered manufacturing in image space. In: Advances in Computers and Information in Engineering Research. ASME Press; 2014.
[6] Huang ZF, Ma YL, Wei JH, Pan AQ, Liu J. Research of fused deposition modeling process oriented component design. Adv Mater Res 2015;1095:828–32.
[7] Meisel NA, Elliott AM, Williams CB. A procedure for creating actuated joints via embedding shape memory alloys in PolyJet 3D printing. J Intell Mater Syst Struct 2015;26(12):1498–512.
[8] Choi JW, Kim HC, Wicker R. Multi-material stereolithography. J Mater Process Technol 2011;211(3):318–28.
[9] Zhou C, Chen Y, Yang Z, Khoshnevis B. Digital material fabrication using mask-image-projection-based stereolithography. Rapid Prototyping J 2013;19(3):153–65.
[10] Sitthi-Amorn P, Ramos JE, Wang Y, Kwan J, Lan J, Wang W, et al. MultiFab: a machine vision assisted platform for multi-material 3D printing. ACM Trans Graphics 2015;34(4):129.
[11] Meisel NA, Williams CB. An investigation of key design for additive manufacturing constraints in multimaterial three-dimensional printing. J Mech Des 2015;137(11):111406.
[12] Pan Y, Zhou C, Chen Y. A fast mask projection stereolithography process for fabricating digital models in minutes. ASME J Manuf Sci Eng 2012;134(5):051011.
[13] Pan Y, Chen Y, Yu Z. Fast mask image projection based micro-stereolithography process for complex geometry. J Micro- Nano-Manuf 2017;5(1):014501.
[14] Venkatasubramanian R, Siivola E, Colpitts T, O'quinn B. Thin-film thermoelectric devices with high room-temperature figures of merit. Nature 2001;413:597–602.
[15] Simons RE, Chu RC. Application of thermoelectric cooling to electronic equipment: a review and analysis. IEEE Sixteenth Annual Semiconductor Thermal Measurement and Management Symposium 2000:1–9.